

Soft-in/Soft-out Noncoherent Sequence Detection for Bluetooth: Capacity, Error Rate and Throughput Analysis

Rohit Iyer Seshadri and Matthew C. Valenti
Lane Dept. of Comp. Sci. & Elect. Eng.
West Virginia University
Morgantown, WV 26506-6109
{iyerr, mvalenti}@csee.wvu.edu

Abstract—This paper investigates an energy efficient, noncoherent system design for Bluetooth. We propose using a soft decision differential phase detector (SDDPD) along with the (15, 10) shortened Hamming channel (SHC) code. Unlike previous work, where SDDPD with ML detection gives hard estimates of the modulated bits, we develop a sequential, soft-in/ soft-out (SISO) SDDPD which exchanges soft information with the channel decoder. The proposed soft decision based receiver gives significant improvements in energy efficiency and throughput over the benchmark Bluetooth receiver using limiter discriminator integrator (LDI) detection with hard decision channel decoding. It also outperforms SDDPD with ML detection followed by hard decision channel decoding. Additional gains are obtained by extending our proposed system to perform bit-interleaved coded modulation (BICM). The effect of bit-interleaving on the performance of LDI detection and SDDPD with hard decision decoding is studied. The capacity of our system under BICM is evaluated and extrinsic information transfer (EXIT) chart analysis is used to analyze convergence behavior of the proposed receiver.

Keywords: Noncoherent receivers, Bluetooth, SDDPD, Hamming codes, LDI, throughput, BICM, capacity, EXIT chart.

I. INTRODUCTION

Gaussian frequency shift keying (GFSK), a class of continuous phase modulation (CPM) [1] is used in the Bluetooth [2] physical layer. Due to memory inherent in GFSK, the optimal coherent receiver uses maximum likelihood (ML) sequence detection [1]. The optimal receiver, as well as low complexity coherent receivers ([3], [4], [5]) are susceptible to phase estimation errors. Noncoherent receivers are hence preferred for Bluetooth systems. The noncoherent detector often used for Bluetooth is the limiter discriminator integrator (LDI) detector [6], [7]. Since the data medium (DM)-rate packet type in Bluetooth is protected by a (15, 10) shortened Hamming channel (SHC) code [2], typically, LDI detection is followed by hard decision decoding (HDD) of the code bits (LDI-HDD). While low in complexity, these receivers have poor energy efficiency, especially in harsh mobile environments. It is hence

desirable to investigate power efficient receiver designs while maintaining feasible complexity.

Lampe et al. proposed a modification to LDI-HDD in [6]. Unlike previous work, [6] exploited both the single and double adjacent error correcting capability of the SHC code which improves performance with a marginal increase in complexity. In [7], a max-log-ML symbol estimation postprocessor was applied at the output of the LDI detector. An uncoded gain of 3.5 dB in E_b/N_o (over conventional LDI detectors) in AWGN for modulation indices $h = 0.28$ and 0.35 was reported. Noncoherent reception for CPM can be improved using sequence detection [8], [9]. A noncoherent sequence detector for Bluetooth was developed in [10] and shown to outperform the max-log-ML LDI detector from [7]. As in [6], the double adjacent error correcting capability of the SHC code was also exploited.

The performance of coded modulation in fading channels can be improved by using a bit-interleaver between the channel encoder and modulator, and by passing bit-wise extrinsic information from the demodulator to the decoder. This is known as *bit-interleaved coded modulation* (BICM) [11]. If the decoder subsequently passes extrinsic information on the coded bits to the demodulator, the resulting scheme is called *BICM with iterative decoding* (BICM-ID) [12], [13], [14], [15].

The noncoherent, soft-decision differential phase detector (SDDPD) with ML detection was introduced by Fonseka in [16]. SDDPD with ML detection was shown to outperform the LDI detector in [17]. In this paper, we investigate coded, noncoherent sequence detection for Bluetooth using SDDPD and the SHC code. Unlike [16] and [17] where SDDPD with ML detection yields hard estimates of the modulated bits followed by HDD by the channel decoder (SDDPD-HDD), we develop a soft-in/soft-out SDDPD (SISO-SDDPD) that generates log-likelihood ratios (LLR) for the modulated bits. Because it is cyclic, the SHC code is treated as a recursive systematic convolutional (RSC) code whose decoder uses bit LLRs from the SISO-SDDPD and gives ML estimates of the information bits, hence performing

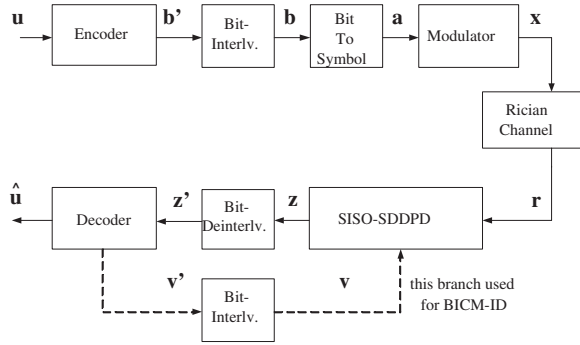


Fig. 1. System model for bit-interleaved coded modulation.

soft decision decoding (SDD). The proposed receiver (denoted as SISO-SDDPD-SDD) gives considerable improvements in error rate and throughput over LDI-HDD and SDDPD-HDD. BICM is investigated using the SISO-SDDPD and the SHC code and is shown to give additional gains over the SISO-SDDPD-SDD. Bit-interleaving is also considered for LDI-HDD and SDDPD-HDD. For SDDPD-HDD, the error rate is seen to improve (especially at higher E_b/N_o) with simple pseudo-random bit-interleaving, but no such gain is observed when using a LDI detector.

The BICM capacity [11] for our system is calculated. BICM-ID is also investigated by replacing a ML channel decoder with a maximum a posteriori (MAP) [18] decoder. Performance and complexity trade-offs for our proposed system are discussed. EXIT chart analysis [19] is used as a convenient tool to analyze convergence behavior of our receiver.

II. SYSTEM MODEL

The system model for BICM is shown in Fig. 1. This is simply the SISO-SDDPD-SDD with bit-interleaving and deinterleaving.

A. Transmitter and Channel

A vector $\mathbf{u} \in \{0, 1\}^{K_u}$ of message bits is passed through the binary encoder to produce a codeword $\mathbf{b}' \in \{0, 1\}^N$. For systems with interleaving, \mathbf{b}' is multiplied by a permutation matrix (bit-interleaver) $\mathbf{\Pi}$ to produce the bit-interleaved codeword $\mathbf{b} = \mathbf{b}'\mathbf{\Pi}$. $\log_2 M$ bits (M is the modulation order) of \mathbf{b} are mapped to one of M symbols (natural mapping) to give $\mathbf{a} \in \{\pm 1, \pm 3, \dots, \pm(M-1)\}^L$, where, $L = \lceil N/\log_2 M \rceil$. The M -ary, baseband GFSK signal in the interval $kT \leq t \leq (k+1)T$ is

$$x(t, \mathbf{a}) = \sqrt{P_x} \exp(\sqrt{-1}\varphi(t, \mathbf{a})) \quad (1)$$

where $P_x = E_s/T$ with symbol energy E_s and symbol period T . Assuming Z symbol ISI, the phase of the GFSK signal can be written as [20]

$$\varphi(t, \mathbf{a}) = \pi h \sum_{i=-\infty}^{k-Z+1} a_i + 2\pi h \sum_{i=k-Z}^{k-1} a_i \int_{-\infty}^t g(\tau - iT) d\tau$$

$$+ 2\pi h a_k \int_{-\infty}^t g(\tau - kT) d\tau$$

$g(t)$ is the response of the Gaussian shaping filter to a rectangular pulse of duration T considered here as,

$$g(t) = [Q(-cB_g t) - Q(-cB_g(t-T))]/T$$

where, $c = 7.546$ and $B_g T$ is the normalized 3 dB bandwidth of the filter and h is the modulation index. The Q function is given by

$$Q(x) = (2\pi)^{-1/2} \int_x^{\infty} \exp(-y^2/2) dy$$

For Bluetooth, $M = 2$, $T = 10^{-6}$ sec, $B_g T = 0.5$, $0.28 \leq h \leq 0.35$ and $Z = 2$. The channel is assumed to be Rician and frequency nonselective and the signal at its output is

$$r(t, \mathbf{a}) = c(t)x(t, \mathbf{a}) + n(t) \quad (2)$$

where,

$$c(t) = \sqrt{P_s} + \sqrt{P_d}\xi(t) \quad (3)$$

P_s is the power gain of the direct signal component, P_d is the power gain of the diffused component, and the Rician K -factor is given by $K = P_s/P_d$. P_s and P_d are normalized such that $P_s + P_d = 1$. $\xi(t)$ is a zero mean, complex Gaussian fading process with variance $1/2$ in each complex dimension. Lastly, $n(t)$ is additive, zero-mean, complex white Gaussian noise with power spectral density $N_o/2$. $r(t, \mathbf{a})$ is passed through a front end receiver filter (not shown in Fig. 1) that removes out of band noise. The phase of the filtered signal can be written as

$$\phi(t, \mathbf{a}) = \varphi(t, \mathbf{a}) + \eta(t) \quad (4)$$

where the phase noise $\eta(t)$ is as defined in [21]. The filtered signal is then passed to the SISO-SDDPD.

B. SISO-SDDPD

As in [16], the SDDPD finds the phase difference between successive symbol intervals as

$$\Delta\phi_k = (\Delta\varphi_k + \eta(t_k) - \eta(t_k - T)) \bmod 2\pi, \quad (5)$$

for $k = 0, 1, \dots, L-1$. Since $Z = 2$

$$\Delta\varphi_k = a_k\theta_0 + a_{k-1}\theta_1 + a_{k+1}\theta_{-1} \quad (6)$$

where

$$\theta_i = \pi h \int_{iT}^{iT+T} g(t) dt$$

From (6), $\Delta\varphi_k$ will have one of $M^{Z+1} = 8$ possible values. The phase region between $0-2\pi$ is divided into R sub-regions. The detector finds one of the R possible sub-regions (D_k), in which $\Delta\phi_k$ lies. The sequence of sub-regions $\mathbf{D} = (D_0, D_1, \dots, D_{L-1})$ is then sent to a branch metric calculator. Let

$\Delta\varphi^i = (\Delta\varphi_0^i, \Delta\varphi_1^i, \dots, \Delta\varphi_{L-1}^i)$ be the phase differences corresponding to any transmitted sequence $\mathbf{a}^i = (a_0^i, a_1^i, \dots, a_{L-1}^i)$. The branch metric calculator finds the conditional probabilities of receiving \mathbf{D} , given $\Delta\varphi^i$ i.e. $P(\mathbf{D}|\Delta\varphi^i)$. The metric for the i^{th} path in the trellis at a symbol interval k from [16] is

$$\begin{aligned} P(D_k|\Delta\varphi_k^i) &= P(\varrho_k^1 \leq \Delta\varphi_k^i < \varrho_k^2) \\ &= 1 + F(\varrho_k^2|\Delta\varphi_k^i) - F(\varrho_k^1|\Delta\varphi_k^i), \varrho_k^1 \leq \Delta\varphi_k^i < \varrho_k^2 \\ &= F(\varrho_k^2|\Delta\varphi_k^i) - F(\varrho_k^1|\Delta\varphi_k^i), \text{otherwise.} \end{aligned} \quad (7)$$

ϱ_k^1 and ϱ_k^2 are the boundaries of the sub-region D_k . The nonlinear function F can be derived from in [21]. The SISO-SDDPD estimates the LLR (z_k) for a_k as

$$z_k = \log \frac{\sum_{A+} \alpha_{k-1}(s') \gamma_k(s', s) \beta_k(s)}{\sum_{A-} \alpha_{k-1}(s') \gamma_k(s', s) \beta_k(s)} \quad (8)$$

where, α , β and γ are the metrics in the MAP/BCJR algorithm [18]. The decoding proceeds on a 4-state trellis whose previous state is $S_{k-1} = (a_{k-1}, a_k)$ and present state is $S_k = (a_k, a_{k+1})$. $A+$ is the set of state transitions $\{S_{k-1} = s'\} \rightarrow \{S_k = s\}$ corresponding to $a_k = +1$ and $A-$ is defined similarly for $a_k = -1$. Also

$$\gamma_k(s', s) = p(a_k|\mathbf{z}\setminus z_k)P(D_k|\Delta\varphi_k)$$

Note that the a priori information to the detector $p(a_k|\mathbf{z}\setminus z_k)$ is generated by the decoder using information pertaining to all symbols excluding z_k i.e. $\mathbf{z}\setminus z_k$. Using a computationally efficient log-domain version of the MAP algorithm [22], the LLR is now

$$z_k = \max_{A+} * \left[\tilde{\alpha}_{k-1}(s') + \tilde{\gamma}_k(s', s) + \tilde{\beta}_k(s) \right] - \quad (9)$$

$$\max_{A-} * \left[\tilde{\alpha}_{k-1}(s') + \tilde{\gamma}_k(s', s) + \tilde{\beta}_k(s) \right]$$

Where, $\tilde{\alpha}$, $\tilde{\gamma}$ and $\tilde{\beta}$ are logarithms of α , γ and β respectively and the $\max *$ operator is defined in [22].

In the SISO-SDDPD-SDD, the channel decoder uses \mathbf{z} to form ML estimates ($\hat{\mathbf{u}}$) of \mathbf{u} . For BICM, the ML decoder uses deinterleaved LLRs \mathbf{z}' ($\mathbf{z}' = \mathbf{z}\mathbf{\Pi}^{-1}$), to generate $\hat{\mathbf{u}}$. Since the SHC code is equivalent to a constraint length 6, RSC code [2], a ML or MAP channel decoder has a 32-state trellis. The BICM-ID receiver iterates between the demodulator (SISO-SDDPD) and the decoder. The deinterleaved extrinsic information from the demodulator \mathbf{z}' is fed to the channel decoder which produces extrinsic information \mathbf{v}' for the code bits. \mathbf{v}' after interleaving becomes the a priori input \mathbf{v} to the demodulator, where

$$v_k = \log \frac{p(a_k = +1|\mathbf{z}\setminus z_k)}{p(a_k = -1|\mathbf{z}\setminus z_k)}$$

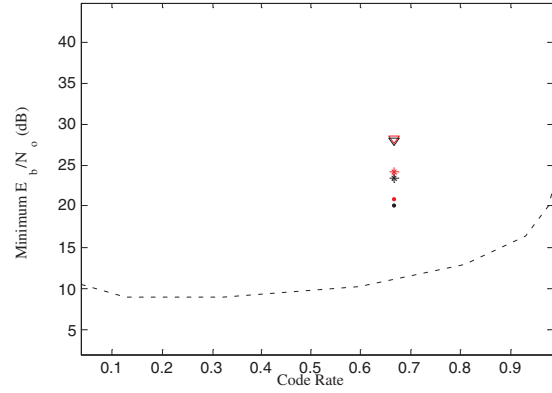


Fig. 2. Dotted curve is the BICM capacity in Rician channel with $K = 2$ dB, using SISO-SDDPD. Six simulated points are shown for DM1 packets, representing minimum E_b/N_o (dB) to achieve BER = 10^{-4} , from top to bottom: (1) LDI-HDD (2) LDI-HDD with bit-interleaving (3) SDDPD-HDD (4) SDDPD-HDD with bit-interleaving (5) SISO-SDDPD-SDD (6) BICM receiver. All SDDPD systems use $R = 24$ uniform phase regions. Modulation index $h = 0.315$ is assumed.

III. BICM CAPACITY

BICM transforms any M -ary modulated system into a set of $\log_2 M$ parallel binary channels [11]. The capacity of the BICM system is the sum of the capacities of these equivalent binary channels. After some manipulation, the ergodic BICM capacity under the constraint of SISO-SDDPD demodulation is

$$C = \log_2 M -$$

$$E_{a,c,n,s' \rightarrow s} \left[\sum_{i=1}^{\log_2 M} \log_2 (1 + \exp(z_i(-1)^{b_i})) \right] \quad (10)$$

E denotes the expectation operation, which is performed over all possible symbols a , fading coefficients c , noise n and state transitions $s' \rightarrow s$. It is assumed that the fading coefficient c remains constant over the duration of a state transition $s' \rightarrow s$. This is evaluated using Monte-Carlo simulations. The bottom most curve in Fig. 2 is the information theoretical minimum E_b/N_o required to achieve arbitrarily low bit error rate (BER) for a BICM receiver using SISO-SDDPD with $R = 24$ uniform phase sub-regions (i.e. width of each sub-region is $2\pi/R$). The channel is Rician with $K = 2$ dB and a modulation index of $h = 0.315$ is assumed. Also shown are the simulated, minimum E_b/N_o for DM1 packet types ($N = 240$) at BER = 10^{-4} and select receivers (BER is measured at the channel decoder's output). The BICM receiver performs closest to capacity. A BER gain of 8 dB and 4.35 dB over LDI-HDD, and SDDPD-HDD respectively and 0.8 dB over the SISO-SDDPD-SDD is observed. BICM-ID was also investigated. However, iterating between the demodulator and decoder gave no significant gain over BICM (hence not shown in Fig. 2). A possible reason could be that $B_g T = 0.5$ causes only a little adjacent

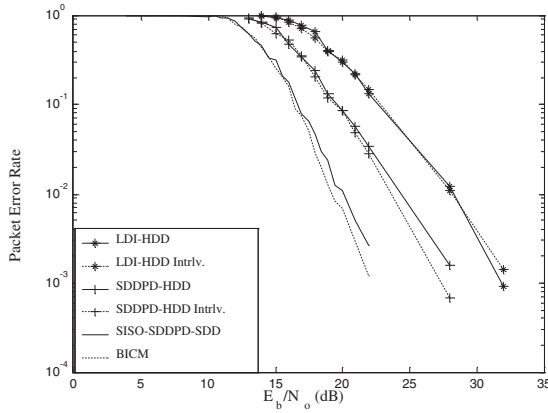


Fig. 3. PER for DM1 packet types in Rician channel with $K = 2$ dB. All SDDPD systems use $R = 24$ uniform phase regions. Dotted curves indicate systems with bit-interleaving. Modulation index $h = 0.315$ is assumed.

symbol interference. Hence during BICM-ID, extrinsic information for each modulated bit is provided by only two other bits, which appears to be insufficient to give noticeable improvement over BICM. Simulations (not shown here) reveal increasing gain using BICM-ID with decreasing values of B_gT . There is however a 9 dB gap between BICM capacity and the proposed receiver. This is primarily due to the short packet sizes and weak channel code used in the Bluetooth standard. This gap could be reduced by using capacity approaching channel codes, such as turbo [23] or LDPC [24] codes instead. It is observed from the capacity curve that the minimum E_b/N_o does not necessarily improve with decreasing code rate. This is due to the noncoherent combining penalty which was also reported in [25].

IV. ERROR RATE, THROUGHPUT AND COMPLEXITY

Extensive simulations were carried out to evaluate the packet error rate (PER) and throughput performance of SISO-SDDPD-SDD and BICM receivers. Comparisons were made with LDI-HDD and SDDPD-HDD, both considered with and without pseudo-random bit-interleaving. In all simulations 100 packet errors were logged at each E_b/N_o . A Rician K factor of 2 dB, and modulation index $h = 0.315$ were assumed. All SDDPD systems utilized $R = 24$ uniform phase regions.

A. Packet Error Rate Performance

Fig. 3 shows the packet error rate (PER) of the DM1 packet type using different receivers. The SISO-SDDPD-SDD receiver gives an E_b/N_o gain of about 8 dB over the LDI-HDD (the SHC code is treated as a single error correcting code). Bit-interleaving is seen to offer no improvement in the PER for LDI-HDD. A 3.1 dB reduction in E_b/N_o is observed compared to SDDPD-HDD. Note that for the SDDPD-HDD, bit-interleaving improves the PER, especially at higher E_b/N_o . BICM gives a 0.82 dB gain over SISO-SDDPD-SDD, this gain was close to 1 dB for the DM3 packet

type and 1.5 dB for the DM5 packet type. BICM-ID was performed with 4 iterations carried out between the SISO-SDDPD and the decoder. No significant improvement was observed over a BICM receiver. Similar gains between receivers were observed for the DM3 and DM5 packet types.

B. Throughput Performance

The throughput (maximum achievable one-way data rate) for the six ACL packets using ARQ (DM1, DM3, DM5, DH1, DH3, DH5) was calculated in [26]. However, [26] assumes nonorthogonal, full response FSK which does not account for GFSK induced ISI. Here, we extend analysis in [26] to find throughput as a function of E_b/N_o for GFSK with Bluetooth specifications, taking into account both ISI and receiver implementation. We consider those ACL packets that use the SHC code (DM1, DM3, DM5). Let N_t be the (average) total number of times a given packet must be transmitted until it is successfully decoded. The data rate (throughput) is a function of N_t given by [26]

$$D_r = \frac{K_p}{(N_s N_t)(625 \times 10^{-6})} \quad (11)$$

where N_s is the number of slots occupied per round trip including one return slot, K_p is the number of data bits in the packet type. Assuming no upper limit of retransmissions,

$$N_t = \frac{1}{1 - \bar{P}e}$$

where $\bar{P}e$ is the average PER. Fig. 4 shows throughput performance for the different receivers for the DM1 packet type. Since relative performance between receivers for the DM3 and DM5 packet type follows a similar trend, only the best (BICM and SISO-SDDPD-SDD) and worst case (LDI-HDD) throughput is shown. At high SNR, the throughput converges to the maximum possible value for each packet type i.e. 108.8 kbps for DM1, 387.2 kbps for DM3 and 477.9 kbps for DM5. The increase in data rate and energy efficiency due to SISO-SDDPD-SDD is evident from Fig. 4. As an example, at $E_b/N_o = 20$ dB, our proposed receiver gives a 30 kbps improvement in throughput over LDI-HDD for DM1 packet types. The gain in throughput is even more significant (450 kbps) at $E_b/N_o = 20$ dB, if DM5 packet types (with SISO-SDDPD-SDD/BICM) were used instead of DM1. Hence, it could be inferred that to achieve maximal throughput, the packet type should be adaptively selected to match the SNR as suggested in [27]. BICM is seen to offer a 5 kbps increase in throughput over SISO-SDDPD-SDD at lower E_b/N_o for the DM1 packet type, and increasing gains are seen with DM3 and DM5 packet types.

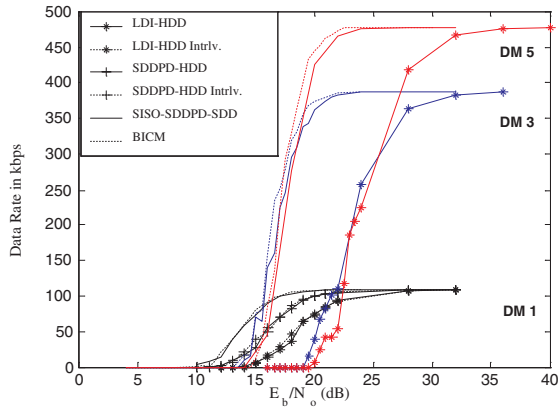


Fig. 4. Throughput for DM1, DM3 and DM5 packet types in Rician channel with $K = 2$ dB. SDDPD systems use $R = 24$ uniform phase regions. Dotted curves indicate systems with bit-interleaving. Modulation index $h = 0.315$ is assumed.

C. Receiver Complexity

At this point some important qualifications on our system's complexity must be made. Our noncoherent sequence detector performs MAP decoding on a 4-state trellis. Prior to MAP decoding, the branch metrics (7) are calculated and stored in an $8 \times R$ look-up table. The metric calculations involve nonlinear functions [17] and need to be updated once at each E_b/N_o making our system more complex than LDI detection. However, it has been pointed out in [3] that branch metrics calculated at $\text{BER} = 10^{-4}$ seem optimum for all E_b/N_o . ML/ MAP decoding of the SHC is performed on a 32-state trellis making it more complex than syndrome decoding used in HDD. The size of the look-up table could be reduced further by careful selection of the phase sub-regions. For simplicity, R uniformly spaced regions are used, but as mentioned in [3], the same performance could be obtained using a smaller number of non-uniform phase regions. However, the non-uniform regions may have to be recalculated each time h changes.

D. Sensitivity to h estimation errors

In Bluetooth, h can take on a range of values ($0.28 \leq h \leq 0.35$), hence, an incorrect estimate could affect the receiver performance. The effect of incorrect estimates of h on SISO-SDDPD and LDI detector is studied in Fig. 5. We consider three cases, 1) the correct value of $h = 0.315$ is known, 2) $h = 0.315$, but receiver assumes a nominal value of $\hat{h} = 0.28$ 3) $h = 0.315$ and receiver assumes $\hat{h} = 0.35$. The SISO-SDDPD is seen to be more robust to incorrect estimates of h than LDI detection. An interesting approach to provide robustness against varying h is to adaptively estimate it before detection as done in [10], though Fig. 5 implies that the additional complexity might not be justified/ necessary for our receiver.

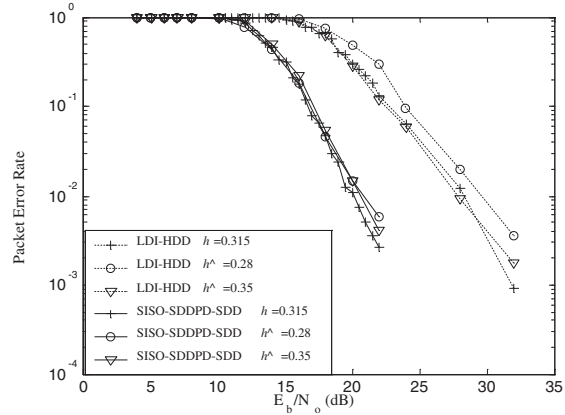


Fig. 5. Effect of incorrect estimates of h on SISO-SDDPD and LDI detector in Rician channel with $K = 2$ dB. SISO-SDDPD ($R = 24$ uniform phase regions) is more robust to incorrect estimates of h than the LDI detector. No bit-interleaving is used in these systems.

V. EXIT CHARTS

In our simulations, we tried iterating between the decoder and demodulator but found that the improvement was negligible. This behavior can be explained in part through EXIT chart analysis [19]. EXIT charts can also be used to predict the convergence threshold (i.e. minimum E_b/N_o to achieve arbitrarily low BER) for our receiver. This involves measuring the bit-wise mutual information (MI) at the outputs of the SISO-SDDPD and the decoder. To start off, the MI at the output of the SISO-SDDPD (I_z) is characterized as a function of E_b/N_o and the MI of the a priori information passed from the decoder (I_v). Histograms from decoder runs reveal \mathbf{v} has Gaussian distribution. If v_k has variance σ_v^2 then the mean is $\sigma_v^2/2$ ($b_k = 1$) or $-\sigma_v^2/2$ ($b_k = 0$). At each value of E_b/N_o and I_v , I_z is calculated by Monte-Carlo simulations.

Fig. 6 shows the extrinsic information transfer characteristics for the SISO-SDDPD at different E_b/N_o . These are essentially straight lines, with two points of interest 1) When $I_v = 0$ (no a priori information at the SISO-SDDPD), hence I_z is the BICM capacity. 2) $I_z = 1$, i.e. perfect a priori knowledge on all bits except a_k , which implies that if the slope of the line is steep, BICM-ID would give significant gains over BICM. In our case, the line is almost horizontal hence implying little/ no benefit over BICM, a result also supported by our error rate simulations. Also, increasing/ decreasing E_b/N_o shifts the curve up/ down. The MI at the output of the decoder ($I_{v'}$) is a function of only $I_{z'}$, where \mathbf{z}' is Gaussian with variance $\sigma_{z'}^2$ and mean $\sigma_{z'}^2/2$ ($b'_k = 1$), or $-\sigma_{z'}^2/2$ ($b'_k = 0$). At each value of $I_{z'}$, $I_{v'}$ is found by Monte-Carlo simulations. The extrinsic information transfer characteristics for the decoder is shown in Fig. 6, note that the curve passes through the point $(0.5, R')$ where $R' = 10/15$ is the code rate. The EXIT chart is obtained by plotting the SISO-SDDPD and decoder characteristics together. The threshold is simply the minimum E_b/N_o at which both curves progress all the

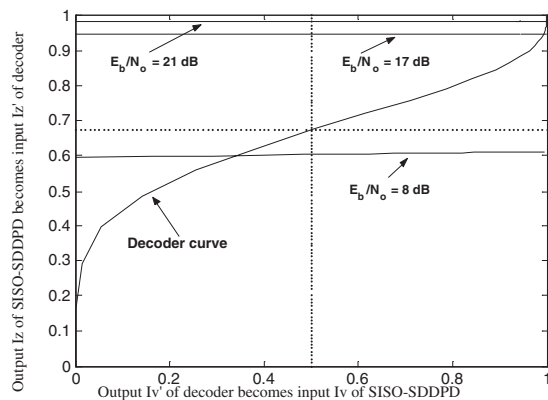


Fig. 6. EXIT chart for the BICM receiver for Bluetooth specifications ($h = 0.315$, $B_g T = 0.5$). SISO-SDDPD EXIT curves assume Rician channel with $K = 2$ dB, $R = 24$ uniform phase regions. Note that the decoder's EXIT curve intersects $(0.5, R')$, where $R' = 10/15$.

way to the right without intersecting. Fig. 6 reveals that the threshold for our receiver is at $E_b/N_o = 21$ dB, which is close to the simulated threshold ($E_b/N_o = 20$ dB) as seen from Fig. 2.

VI. CONCLUSION

An energy efficient, noncoherent receiver design has been investigated for Bluetooth. Towards this end, a MAP based SISO-soft decision differential phase detector is proposed. Improvements in the error rate and throughput are obtained by passing soft information from the detector to the channel decoder. Select simulations reveal close to 8 dB improvement in the packet error rate over the LDI detector and 3.1 dB gain over a ML based SDDPD, both with hard decision decoding by the channel code. Although the Bluetooth standard does not explicitly specify interleaving, we have shown that further improvements in the error rate and throughput are possible by applying the BICM paradigm to our proposed system. The capacity under BICM has been evaluated. Iterating between the detector and decoder is shown to give no improvement over BICM and this conclusion is corroborated by EXIT chart analysis. Our receiver is also shown to be more robust to incorrect estimation of the modulation index than the LDI detector. While the proposed system is more complex than those using LDI detection, it is felt that the significant improvements in error rate and throughput, as well as the potential gains indicated by the BICM capacity make this an interesting proposition for Bluetooth systems.

REFERENCES

- [1] J. B. Anderson, T. Aulin, and C. E. Sundberg, *Digital Phase Modulation*. New York: Plenum Press, 1986.
- [2] Bluetooth Special Interest Group, "Specification of the Bluetooth system," *Core Version 1.2*, Nov. 2003.
- [3] J. P. Fonseka, "Soft-decision phase detection with Viterbi decoding for CPM signals," *IEEE Trans. Commun.*, vol. 47, pp. 1802–1810, Dec. 1999.

- [4] A. Soltanian and R. E. Van Dyck, "Performance of the Bluetooth system in fading dispersive channels and interference," in *Proc. IEEE GLOBECOM Conference*, (San Antonio, TX), pp. 3499–3503, Nov. 2001.
- [5] R. Schiphorst, F. Hoeksema, and C. H. Slump, "A (simplified) Bluetooth maximum a posteriori probability (MAP) receiver," in *Proc. IEEE SPAWC Workshop*, pp. 160–164, Jun. 2003.
- [6] L. Lampe, M. Jain, and R. Schober, "Improved decoding for Bluetooth systems," *IEEE Trans. Commun.*, vol. 53, pp. 1–4, Jan. 2005.
- [7] T. Scholand, A. Waadt, and P. Jung, "Max-log-ML symbol estimation postprocessor for intermediate frequency LDI detectors," *IEE Electronics Letters*, vol. 40, pp. 183–184, Feb. 2004.
- [8] M. K. Simon and D. Divsalar, "Maximum-likelihood block detection of noncoherent continuous phase modulation," *IEEE Trans. Commun.*, vol. 41, pp. 90–98, Jan. 1993.
- [9] J. P. Fonseka, "Noncoherent detection with Viterbi decoding for GMSK signals," *IEE Proc. Commun.*, vol. 143, pp. 373–379, Dec. 1996.
- [10] L. Lampe, R. Schober, and M. Jain, "Noncoherent sequence detection receiver for Bluetooth systems," *IEEE Journ. on Sel. Areas of Commun.*, vol. 23, Sep. 2005.
- [11] G. Caire, G. Taricco, and E. Biglieri, "Bit-interleaved coded modulation," *IEEE Trans. Inform. Theory*, vol. 44, pp. 927–946, May. 1998.
- [12] X. Li and J. A. Ritcey, "Bit-interleaved coded modulation with iterative decoding," *IEEE Commun. Letters*, vol. 1, pp. 169–171, Nov. 1997.
- [13] K. R. Narayanan and G. L. Stüber, "Performance of trellis-coded CPM with iterative demodulation and decoding," *IEEE Trans. Commun.*, vol. 49, pp. 676–687, Apr. 2001.
- [14] P. Moqvist and T. Aulin, "Serially concatenated continuous phase modulation with iterative decoding," *IEEE Trans. Commun.*, vol. 49, pp. 1901–1915, Nov. 2001.
- [15] M. C. Valenti and S. Cheng, "Iterative demodulation and decoding of turbo coded M-ary noncoherent orthogonal modulation," *IEEE Journ. on Sel. Areas of Commun.*, vol. 23, pp. 1739 – 1747, Sep. 2005.
- [16] J. P. Fonseka, "Soft-decision differential phase detection with Viterbi decoding in satellite mobile systems," *Jrn. of Commun. and Netw.*, pp. 265–272, Sept. 2001.
- [17] R. I. Seshadri, D. Lao, C. Kwan, and J. P. Fonseka, "Bandwidth constrained, low complexity noncoherent CPM with ML soft-decision differential phase detection," in *Proc. IEEE MILCOM Conference*, (Atlantic City, NJ), Oct. 2005.
- [18] L. Bahl, J. Cocke, F. Jelinek, and J. Raviv, "Optimal decoding of linear codes for minimizing symbol error rate," *IEEE Trans. Inform. Theory*, vol. 20, pp. 284–287, Mar. 1974.
- [19] S. ten Brink, "Convergence of iterative decoding," *IEE Electronics Letters*, vol. 35, pp. 1117–1118, Jun. 1999.
- [20] J. Proakis, *Digital Communications*. New York: McGraw-Hill, Inc., fourth ed., 2001.
- [21] I. Korn, "GMSK with differential phase detection in the satellite mobile channel," *IEEE Trans. Commun.*, vol. 38, pp. 1980–1986, Nov. 1990.
- [22] A. Viterbi, "An intuitive justification and a simplified implementation of the MAP decoder for convolutional codes," *IEEE Journ. on Sel. Areas of Commun.*, vol. 16, pp. 260–264, Feb. 1998.
- [23] C. Berrou, A. Glavieux, and P. Thitimajshima, "Near Shannon limit error-correcting coding and decoding: Turbo-codes," in *Proc. IEEE Int. Conf. on Commun.*, vol. 2, (Geneva), pp. 1064–1070, May 1993.
- [24] R. Gallager, "Low-density parity-check codes," *IRE Trans. Inform. Theory*, vol. 8, pp. 21–28, Jan. 1962.
- [25] W. E. Stark, "Capacity and cutoff rate of noncoherent FSK with nonselective Rician fading," *IEEE Trans. Commun.*, vol. 33, pp. 1153–1159, Nov. 1985.
- [26] M. C. Valenti, M. Robert, and J. H. Reed, "On the throughput of bluetooth data transmissions," in *Proc. IEEE Wireless Commun. and Networking Conf.*, (Orlando, FL), pp. 119–123, Mar. 2002.
- [27] M. C. Valenti and M. Robert, "Custom coding, adaptive rate control, and distributed detection for bluetooth," in *Proc. IEEE Vehicular Tech. Conf.*, pp. 927–931, Sep. 2002.